



# Nitric oxide and Nitrous oxide accumulation, oxygen production during nitrite denitrification in an anaerobic/anoxic sequencing batch reactor: exploring characteristics and mechanism

Sha Wang<sup>1,2</sup> · Bin Li<sup>1</sup> · Fang Li<sup>1,2</sup>

Received: 11 October 2022 / Accepted: 15 December 2022 / Published online: 21 December 2022  
© The Author(s), under exclusive licence to Springer-Verlag GmbH Germany, part of Springer Nature 2022

## Abstract

Nitrite denitrification has received increasing attention due to its high efficiency, low energy consumption, and sludge yield. However, the nitric oxide (NO) and nitrous oxide (N<sub>2</sub>O) which are harmful to the environment, microorganisms, and humans are produced in this process. In order to mitigate NO and N<sub>2</sub>O production, the biological mechanisms of NO and N<sub>2</sub>O accumulation, as well as NO detoxification during nitrite denitrification in a sequencing batch reactor were studied. Results showed that the peak of NO accumulation increased from  $0.29 \pm 0.01$  to  $3.12 \pm 0.34$  mg L<sup>-1</sup> with the increase of carbon to nitrogen ratio (COD/N), which is caused by the sufficient electron donor supply for NO<sub>2</sub><sup>-</sup>-N reduction process at high COD/N. Furthermore, the result suggested that NO accumulation with no pH adjustment was 12 times higher than that with pH adjustment. It is related to the inhibition on NO reductase caused by the high free nitrous acid (FNA) and NO concentration with no pH adjustment. The pathways of NO detoxification included NO emission, reduction, and dismutation, and the more NO produced, the high proportion of NO dismutation pathway. Result showed that the maximum of oxygen production during NO dismutation reached to 1.39 mg L<sup>-1</sup>. N<sub>2</sub>O accumulation was mainly associated with FNA and NO inhibition, COD/N. The peak of N<sub>2</sub>O accumulation presented a completely opposite trend at pH adjustment and no pH adjustment, it is because that the higher FNA and NO concentration at high COD/N without pH adjustment will inhibit the N<sub>2</sub>O reductase activity, resulting in the N<sub>2</sub>O reduction was hindered during nitrite denitrification.

**Keywords** Nitric oxide · Nitrous oxide · Nitrite denitrification · NO detoxification · NO dismutation · NO inhibition · FNA inhibition

---

Responsible Editor: Guilherme L. Dotto

## Highlights

NO and N<sub>2</sub>O accumulation was caused by imbalanced electron distribution.  
NO detoxification was achieved by NO emission, reduction and dismutation.  
The high DO concentration of 1.39 mg L<sup>-1</sup> was produced during NO dismutation.

---

✉ Sha Wang  
sand368@126.com

<sup>1</sup> College of Environment and Life Sciences, Weinan Normal University, Weinan 714099, Shaanxi, China

<sup>2</sup> Key Laboratory for Ecology and Environment of River Wetlands in Shaanxi Province, Weinan 714099, Shaanxi, China

## Introduction

With the rapid development of industry and agriculture, a large amount of wastewater containing nitrogen-compounds are discharged into surface water, causing serious eutrophication of water body. In order to control the increasing nitrogen pollution, various technologies, such as physical, chemical, and biological methods, have been developed and applied in wastewater treatment (Hossini et al. 2015; Dehghani et al. 2018; Jonoush et al. 2020). Among them, biological nitrogen removal (BNR) is widely used due to its high efficiency and low cost. BNR is performed by aerobic nitrification and anoxic denitrification. In the nitrification process, ammonia (NH<sub>4</sub><sup>+</sup>-N) is first oxidized to nitrite (NO<sub>2</sub><sup>-</sup>-N) and then to nitrate (NO<sub>3</sub><sup>-</sup>-N). Subsequently, the NO<sub>3</sub><sup>-</sup>-N is reduced to nitrogen (N<sub>2</sub>) in the denitrification process. However, for some types of wastewater, such as landfill leachate, anaerobic

digester liquor, and aquaculture wastewater,  $\text{NH}_4^+\text{-N}$  can only be oxidized to  $\text{NO}_2^-\text{-N}$  due to the complex composition and inhibition of toxic substances. Therefore, the nitrite denitrification is performed to reduce the  $\text{NO}_2^-\text{-N}$  to  $\text{N}_2$ . Compared with conventional denitrification, nitrite denitrification has a fast reaction rate (1.5~2 times faster), and can theoretically save 40% of carbon oxygen demand (COD), resulting in 20% less carbon dioxide emission and 30~50% less sludge production (Dobbeleers et al. 2018).

However, research showed that some unexpected intermediates, like nitric oxide (NO) and nitrous oxide ( $\text{N}_2\text{O}$ ), were accumulated in nitrite denitrification process (Wang et al. 2019a).  $\text{N}_2\text{O}$  is a powerful greenhouse gas with a steady-state lifetime of 114 years in the atmosphere, its greenhouse effect is 310 and 9.5 times higher than that of carbon dioxide ( $\text{CO}_2$ ) and methane ( $\text{CH}_4$ ), respectively (IPCC 2013). In addition,  $\text{N}_2\text{O}$  can react with the ozone in the stratosphere, resulting in the ozone depletion. At the same time, NO as another important intermediate in the nitrite denitrification, can also cause a series of serious environmental problems, including acid rain, ozone hole, and photochemical smog (Adouani et al. 2010). Furthermore, NO is a potent toxic gas that can exert severe effects on the metabolism of bacteria, prokaryotes, and eukaryotes (Wang et al. 2016), causing a low removal efficiency of pollutants. Schulthess et al. (1995) found that dissolved NO concentration of  $0.6 \text{ mg L}^{-1}$  could inhibit the reductases involved in nitrite denitrification, leading to a low conversion rate (Schulthess et al. 1995). Adouani et al. (2010) also reported that  $\text{N}_2\text{O}$  reductase (Nos) was inhibited by NO, resulting in high  $\text{N}_2\text{O}$  accumulation. Therefore, the study on NO inhibition and detoxication also play a significant role in the nitrite denitrification, and it is imperative to explore the mechanism of NO and  $\text{N}_2\text{O}$  accumulation in the nitrite denitrification and propose mitigation measurements.

Conventionally, when NO was accumulated during denitrification, microorganism will reduce NO to  $\text{N}_2\text{O}$ , and then to  $\text{N}_2$  to mitigate the toxicity. However, a novel pathway for NO detoxication, NO could be dismutated to  $\text{N}_2$  and  $\text{O}_2$ , was reported in recent research (Ettwig et al. 2010). This process is catalyzed by NO dismutase (Nod), and no  $\text{N}_2\text{O}$  is produced. Furthermore, external electron is not required in NO dismutation (Eq. (1)). Thus, NO dismutation is an attractive alternative to reduction of NO to  $\text{N}_2\text{O}$  in canonical denitrification process. According to previous research, NO dismutation occurred only in nitrite-driven anaerobic methane oxidation (n-DAMO) process, which was rarely reported in nitrite denitrification. Therefore, in order to explore NO dismutation in the nitrite denitrification, further research is needed regarding the NO accumulation and detoxication in this process.



The carbon to nitrogen ratio (COD/N) play an important role in nitrite denitrification process (Wang et al. 2019b), which has significant impact on NO and  $\text{N}_2\text{O}$  production. In addition, the high NO and  $\text{N}_2\text{O}$  production of  $0.67 \pm 0.06$  and  $9.03 \pm 1.02 \text{ mg L}^{-1}$  occurred when glucose was used as carbon source for denitrification. However, the mechanism of COD/N on NO and  $\text{N}_2\text{O}$  production, NO inhibition and detoxication in nitrite denitrification with acetate as a carbon source was not referred before. Therefore, in the present study, the NO and  $\text{N}_2\text{O}$  accumulation, as well as NO detoxication in the nitrite denitrification with acetate as a carbon source was investigated. The main objectives were to (1) illustrate the characteristic of NO and  $\text{N}_2\text{O}$  accumulation under different COD/N; (2) explore the mechanism of NO and  $\text{N}_2\text{O}$  accumulation; (3) demonstrate the pathway of NO detoxication.

## Materials and methods

### Reactor setup and operation

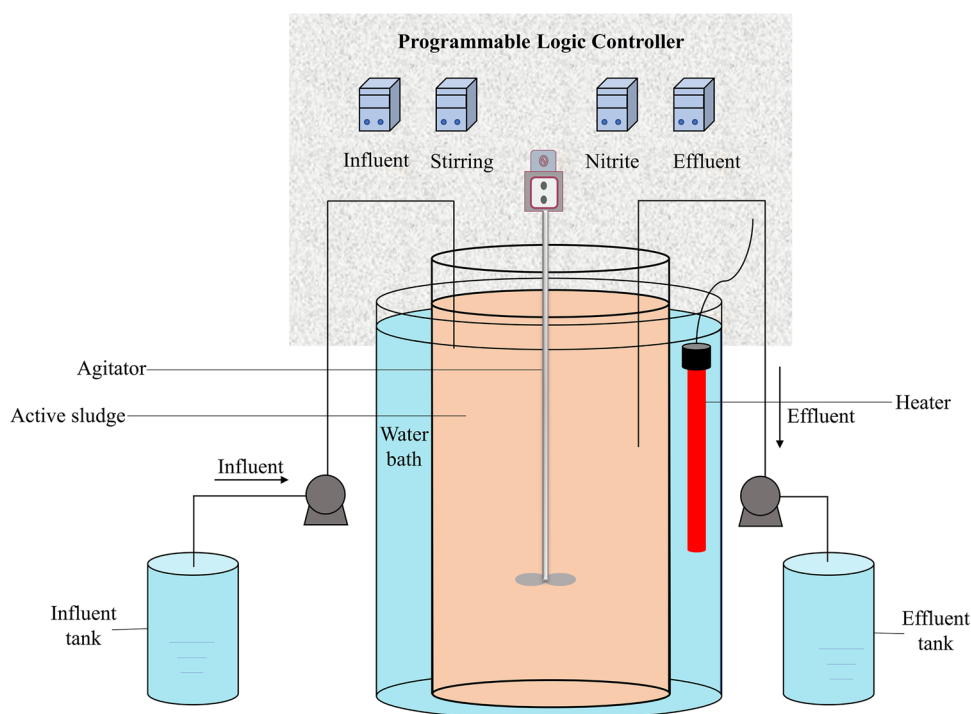
A lab-scale nitrite denitrifying sequencing batch reactor (SBR) was supplied by acetate as carbon source with an effective volume of 8 L was applied in this study (Fig. 1). The SBR was made of plexiglass with identical dimensions of 41 cm in height and 24 cm in diameter. The influent, effluent, and stir were controlled automatically by a programmable logic controller (PLC). The seed sludge was collected from the anoxic pond in a municipal wastewater treatment plant in Xi'an, China. The reactor was operated at  $30 \pm 1 \text{ }^\circ\text{C}$  with a cycle time of 240 min, which consisted of 5 min feeding, 60 min anaerobic stage, 100 min anoxic stage, 35 min settling, and 40 min decanting. In each cycle, 3 L synthetic wastewater was pumped into the reactor by a submerged pump at the beginning of the anaerobic phase, and 0.1 L  $\text{NaNO}_2$  was added into the reactor after a 60-min anaerobic stage. During the stable operation, a 0.1-L mixed liquor was discharged at the end of the anoxic stage, achieving a solids retention time (SRT) of approximately 13 days and a mixed liquor volatile suspended solid (MLVSS) of  $3502 \pm 123 \text{ mg L}^{-1}$ . The initial pH of the mixed liquor was controlled at  $7.5 \pm 0.5$  by a pH meter (PHS-3C, China).

The reactor achieved a steady state after approximately 3 months of operation, and the removal efficiency of COD and  $\text{NO}_2^-\text{-N}$  were higher than 90%.

### Synthetic wastewater

The synthetic wastewater contained:  $1.92 \text{ mL L}^{-1}$   $\text{CH}_3\text{COOH}$  ( $270 \text{ mg L}^{-1}$  COD),  $443.57 \text{ mg L}^{-1}$   $\text{NaNO}_2$

**Fig. 1** Experimental schematic of the SBR



(90 mg L<sup>-1</sup> NO<sub>2</sub><sup>-</sup>-N), 16.46 mg L<sup>-1</sup> KH<sub>2</sub>PO<sub>4</sub>, 41 mg L<sup>-1</sup> CaCl<sub>2</sub>, and 1 mL L<sup>-1</sup> trace element solution. The trace element solution consisted of: 10 g L<sup>-1</sup> C<sub>10</sub>H<sub>14</sub>N<sub>2</sub>Na<sub>2</sub>O<sub>8</sub>·2H<sub>2</sub>O, 0.15 g L<sup>-1</sup> CoCl<sub>2</sub>·6H<sub>2</sub>O, 0.03 g L<sup>-1</sup> CuSO<sub>4</sub>·5H<sub>2</sub>O, 0.15 g L<sup>-1</sup> H<sub>3</sub>BO<sub>3</sub>, 0.18 g L<sup>-1</sup> KI, 0.12 g L<sup>-1</sup> MnCl<sub>2</sub>·4H<sub>2</sub>O, 0.06 g L<sup>-1</sup> Na<sub>2</sub>MoO<sub>4</sub>·2H<sub>2</sub>O, and 0.12 g L<sup>-1</sup> ZnSO<sub>4</sub>·7H<sub>2</sub>O.

### Batch tests

The batch tests were performed in the anaerobic/anaerobic (An/A) SBR. Six tests were conducted in this study with triplicates (Table S1). At the beginning of each test, different levels of CH<sub>3</sub>COOH were pumped into the reactor to achieve initial COD concentrations of 90, 270, 360, and 540 mg L<sup>-1</sup>. After a 60-min anaerobic operation, 3.55 g L<sup>-1</sup> NaNO<sub>2</sub> was added into the reactor, resulting in the initial NO<sub>2</sub><sup>-</sup>-N concentration of 90 mg L<sup>-1</sup>. The initial pH was controlled at 7.5 ± 0.5. In batch test 1–4, the pH was not adjusted during the anaerobic stage, resulting in different pH (the pH decreased with the increase of COD/N due to the acidity of acetate) at the beginning of the anoxic stage. Therefore, in order to maintain similar initial pH for denitrification, the pH was adjusted by 0.1 mol L<sup>-1</sup> NaOH solution during the anaerobic stage at tests of 5 and 6 (Table S1), which were defined as 3a and 6a.

### Analysis and measurements

COD, NO<sub>2</sub><sup>-</sup>-N, and MLVSS were measured following the standard methods (APHA 2005). Poly-β-hydroxyalkanoates (PHAs) was determined according to previous study (Jia

et al. 2013). NO and N<sub>2</sub>O accumulation (dissolved NO and N<sub>2</sub>O) were monitored online by the microsensors (Unisense A/S, Aarhus, Denmark) with data logged every 10 s. The NO and N<sub>2</sub>O emission (gaseous NO and N<sub>2</sub>O) were calculated using the method described by Wang et al. (2019a). All statistical analyses were performed using SPSS 19.0.

### Calculations

The FNA concentration was calculated according to the Eq. (2).

$$C = \frac{C_{\text{NO}_2}}{1 + e^{-2300/(273+T)} \times 10^{\text{pH}}} \quad (2)$$

where  $C$  is the FNA concentration, mg L<sup>-1</sup>;  $C_{\text{NO}_2}$  is the NO<sub>2</sub><sup>-</sup>-N concentration, mg L<sup>-1</sup>;  $T$  is the temperature, °C.

The specific denitrification rate was calculated according to the Eq. (3).

$$V = \frac{C_{\text{NO}_2\text{in}} - C_{\text{NO}_2\text{eff}}}{T1 \times C_{\text{MLVSS}}} \times 60 \times 24 \quad (3)$$

where  $V$  is the specific denitrification rate, kg (kg vss)<sup>-1</sup> day<sup>-1</sup>;  $C_{\text{NO}_2\text{in}}$  is the initial NO<sub>2</sub><sup>-</sup>-N concentration, mg L<sup>-1</sup>;  $C_{\text{NO}_2\text{eff}}$  is the NO<sub>2</sub><sup>-</sup>-N concentration in the effluent, mg L<sup>-1</sup>;  $T1$  is the reaction time, min;  $C_{\text{MLVSS}}$  is the MLVSS concentration, mg L<sup>-1</sup>.

The apparent specific  $\text{NO}_2^-$ -N, NO, and  $\text{N}_2\text{O}$  consumption rates were calculated through linear regression of  $\text{NO}_2^-$ -N, NO, and  $\text{N}_2\text{O}$  profiles, respectively. The accumulation represented as negative consumption. The true specific  $\text{NO}_2^-$ -N, NO, and  $\text{N}_2\text{O}$  reduction rates, specific electron consumption rates of nitrite reductase (Nir), NO reductase (Nor), and Nos, as well as electron distribution were calculated according to Pan et al. (2013).

## Results

### Start-up and operation of the reactor

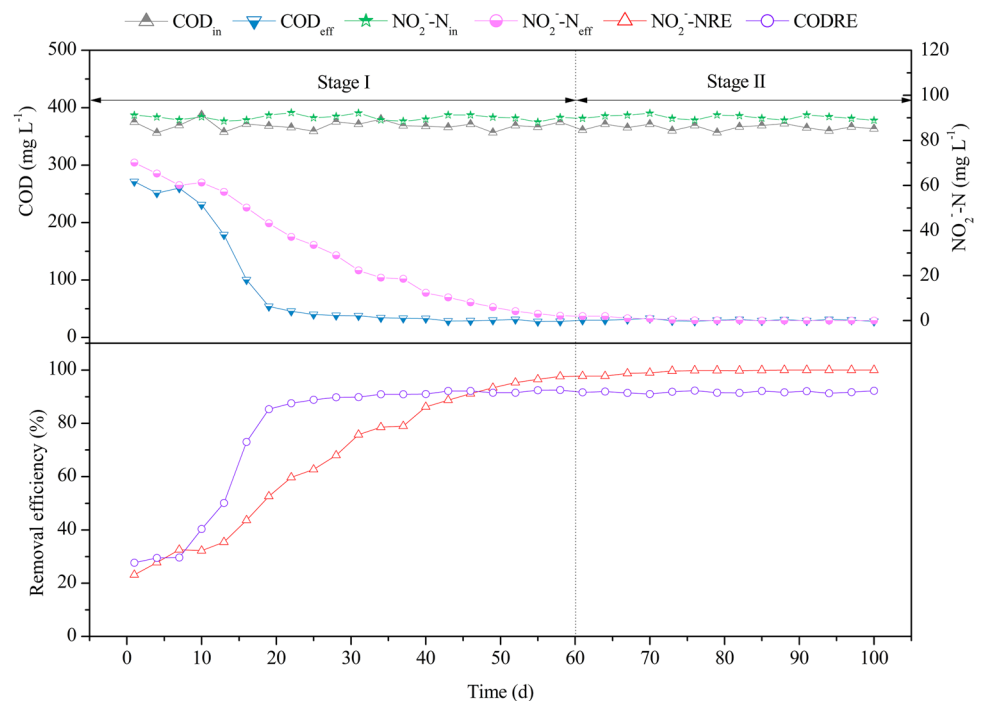
The operation of the An/A SBR could be divided into two stages according to the removal efficiency of COD and  $\text{NO}_2^-$ -N, which were start-up stage (stage I, 1 ~ 60 d) and steady-state stage (stage II, 61 ~ 100 d). As shown in Fig. 2, the effluent COD and  $\text{NO}_2^-$ -N concentrations were high at the beginning of the stage I, resulting in low pollutants removal efficiency of the SBR. However, the COD and  $\text{NO}_2^-$ -N level in the effluent decreased gradually from the 40<sup>th</sup> day, and an excellent pollutant removal performance was achieved in the An/A SBR on day 60. In the stage II, the effluent COD and  $\text{NO}_2^-$ -N value were maintained at approximately  $30.12 \pm 1.21$  and  $0.02 \pm 0.01 \text{ mg L}^{-1}$ , respectively. Accordingly, the removal efficiency of COD and  $\text{NO}_2^-$ -N reached to  $91.45 \pm 1.02$  and  $99.89 \pm 0.11\%$ , respectively. It indicated that a well steady state of the An/A SBR was achieved, and the batch tests could be conducted in the SBR.

### Pollutants removal performance at different COD/N

The COD and  $\text{NO}_2^-$ -N removal efficiency at different COD/N were calculated and the results are shown in Table 1. The COD removal efficiency (CODRE) was only  $69.68 \pm 4.12\%$  under the COD/N of 1, while it was higher than 90% when COD/N were 3, 4, and 6. In addition, the result showed that  $\text{NO}_2^-$ -N removal efficiency ( $\text{NO}_2^-$ -NRE) at different COD/N were higher than 99%, and there was no significant difference among these batch tests, except for the COD/N of 1. However, the specific denitrification rate presented a different variation with  $\text{NO}_2^-$ -N removal performance. As shown in Table 1, the specific denitrification rate increased initially and then decreased when the COD/N increased from 1 to 6 without pH adjustment during the anaerobic stage, and the maximum value of  $0.31 \pm 0.03 \text{ kg (kg vss)}^{-1} \text{ day}^{-1}$  was achieved at COD/N of 3. This phenomenon was different from investigation reported by Fu et al. (2021). On the other hand, the specific denitrification rates at COD/N of 3 and 6 with pH adjustment were approximately 1.13 and 2.05 times higher than that of without pH adjustment respectively. Furthermore, higher specific denitrification rate was achieved at COD/N of 6 when the pH was adjusted during the anaerobic stage. These results suggested that the pH adjustment could significantly improve the denitrification performance, especially at high COD/N level.

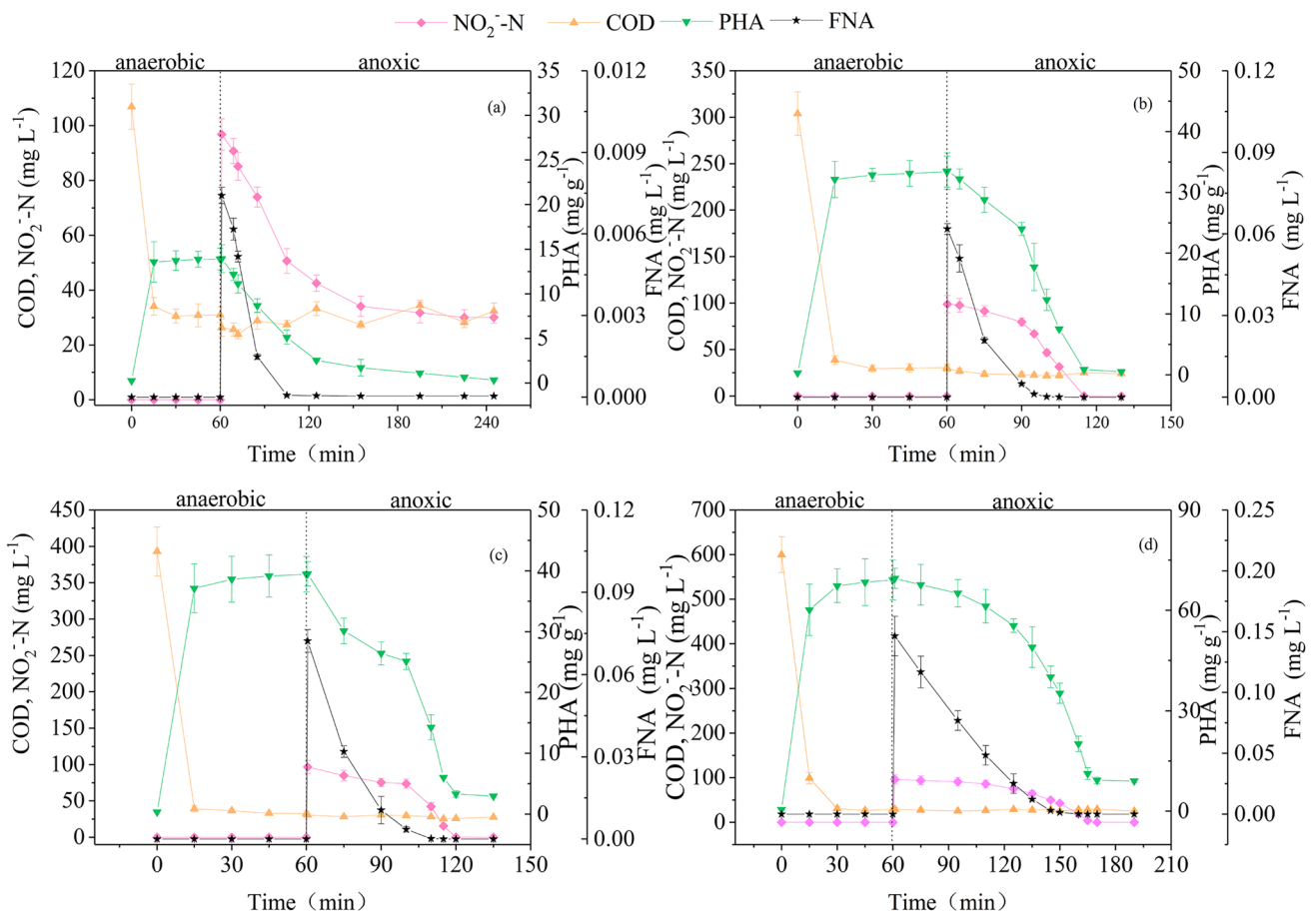
In order to further explore the effect of COD/N on pollutants removal efficiency, the variations of COD and  $\text{NO}_2^-$ -N at different COD/N were investigated. Figures 3 and 4 showed that similar COD transformation tendency occurred

**Fig. 2** The variations of influent, effluent, and removal efficiency during the start-up of SBR



**Table 1** The pollutant removal efficiency and specific denitrification rates at different COD/N

COD/N	Parameters	COD	NO <sub>2</sub> <sup>-</sup> -N
1	Removal efficiency (%)	69.68 ± 4.12	68.97 ± 3.24
	Specific denitrification rate (kg (kg vss) <sup>-1</sup> day <sup>-1</sup> )	0.11 ± 0.01	
3	Removal efficiency (%)	92.07 ± 5.67	99.98 ± 4.89
	Specific denitrification rate (kg (kg vss) <sup>-1</sup> day <sup>-1</sup> )	0.31 ± 0.03	
4	Removal efficiency (%)	92.94 ± 4.09	99.99 ± 4.56
	Specific denitrification rate (kg (kg vss) <sup>-1</sup> day <sup>-1</sup> )	0.29 ± 0.02	
6	Removal efficiency (%)	95.80 ± 5.01	99.98 ± 6.11
	Specific denitrification rate (kg (kg vss) <sup>-1</sup> day <sup>-1</sup> )	0.21 ± 0.01	
3a	Removal efficiency (%)	90.55 ± 4.56	99.98 ± 5.78
	Specific denitrification rate (kg (kg vss) <sup>-1</sup> day <sup>-1</sup> )	0.35 ± 0.04	
6a	Removal efficiency (%)	94.99 ± 3.45	99.96 ± 5.45
	Specific denitrification rate (kg (kg vss) <sup>-1</sup> day <sup>-1</sup> )	0.43 ± 0.05	

**Fig. 3** The pollutant transformations at different COD/N (a) COD/N=1, (b) COD/N=3, (c) COD/N=4, (d) COD/N=6

at all batch tests, namely, the COD concentration decreased rapidly at the beginning of the anaerobic stage (in the first 15 min), and then maintained at a low level during the rest of the test. Notably, when the COD/N was 6, it took 30 min to completely consume the COD. In the anaerobic stage, the COD was stored as PHAs, and then, which was used as

electron donor for endogenous denitrification in the anoxic stage. Therefore, as shown in Figs. 3 and 4, the amount of PHAs synthesis increased with the decrease of COD, and reached to the peak at the end of the anaerobic stage. The amount of PHAs synthesis at different COD/N like 1, 3, 4, 6, 3a, and 6a were  $13.93 \pm 1.56$ ,  $33.51 \pm 3.01$ ,  $39.51 \pm$



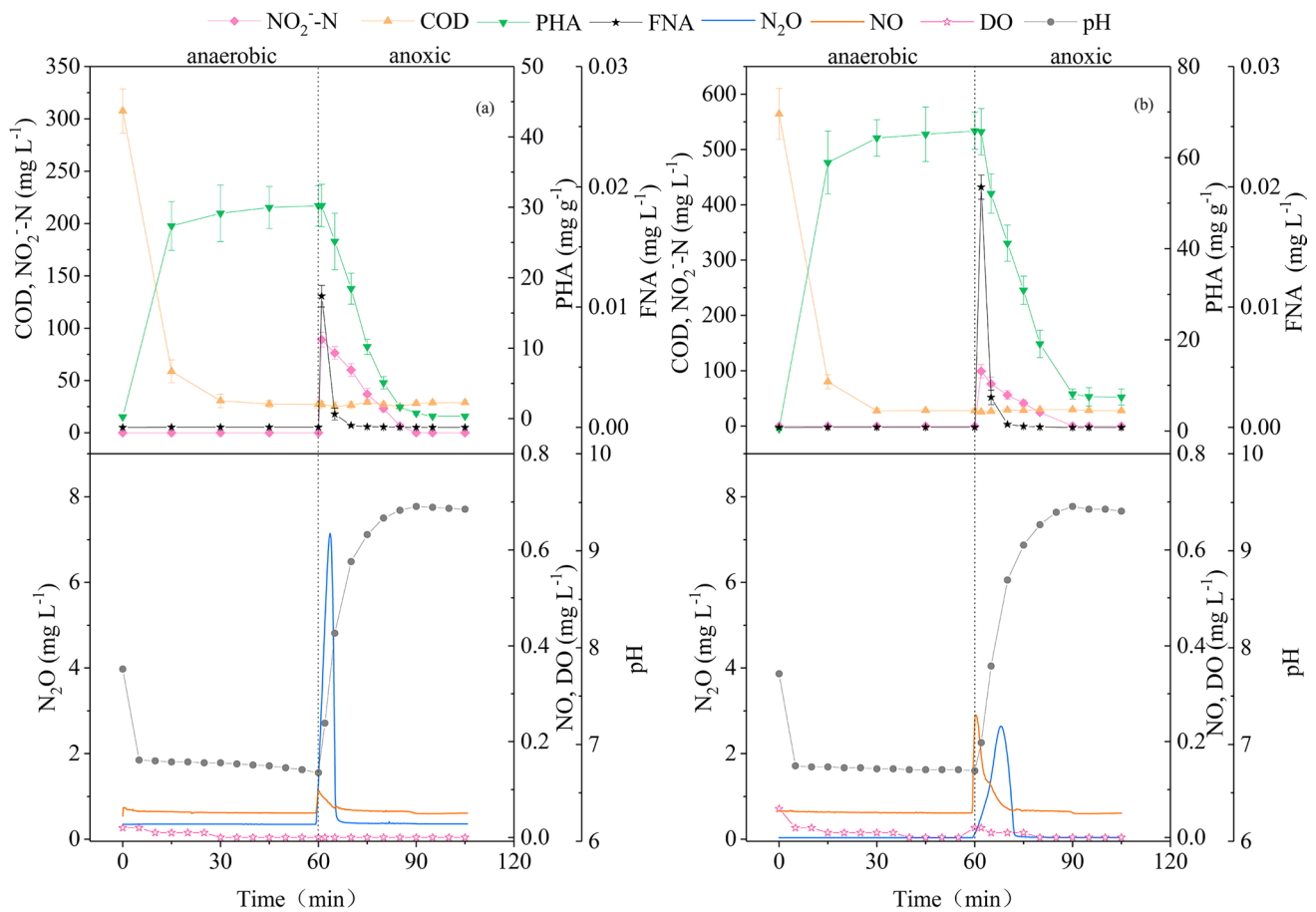


**Fig. 4** The pollutant transformations, NO and N<sub>2</sub>O accumulation at COD/N of 3a and 6a (a) COD/N=3a, (b) COD/N=6a

2.01,  $69.56 \pm 3.22$ ,  $30.25 \pm 2.12$ , and  $65.89 \pm 4.07$  mg g<sup>-1</sup>, respectively. It indicates that high COD/N level is conducive to PHAs synthesis, and the pH adjustment has a slightly effect on PHAs synthesis. In the anoxic stage, the PHAs was consumed gradually as the electron donor for the denitrification, which was stabilized at low level when the NO<sub>2</sub><sup>-</sup>-N was exhausted. However, the PHAs concentration decreased to a very low level even though high NO<sub>2</sub><sup>-</sup>-N concentration was maintained in the reactor due to the insufficient electron donor supply at COD/N of 1.

As shown in Fig. 3, the variation of NO<sub>2</sub><sup>-</sup>-N at different COD/N were different. When COD/N was 1, the NO<sub>2</sub><sup>-</sup>-N decreased quickly in the first 60 min of the anoxic stage, after that, which presented a slow decrease trend. In addition, a total of approximately 30 mg L<sup>-1</sup> NO<sub>2</sub><sup>-</sup>-N was remained in the reactor at the end of the test. At COD/N of 3, 4, and 6, the NO<sub>2</sub><sup>-</sup>-N was consumed slowly at the beginning of the anoxic stage, and then reduced rapidly in a short time. Result showed that the duration of slow consumption increased from 30 to 65 min with the increase of COD/N. Furthermore, it was calculated that the NO<sub>2</sub><sup>-</sup>-N consumption rates at the beginning of the anoxic stage (in the first 30 min)

at different COD/N (1, 3, 4, 6) were 57.32, 40.21, 38.58, and 12.01 mg L<sup>-1</sup> h<sup>-1</sup>, respectively. However, when the pH was adjusted during the anaerobic stage, the NO<sub>2</sub><sup>-</sup>-N consumption rate increased significantly, and the higher COD/N resulted in the faster level of the NO<sub>2</sub><sup>-</sup>-N reduction. It suggested that the endogenous denitrification was not only significantly affected by COD/N, but also by pH.

### NO and N<sub>2</sub>O production at different COD/N

The variation of NO and N<sub>2</sub>O accumulation at different COD/N were investigated and the results are shown in Fig. 4. During the anaerobic stage, negligible NO and N<sub>2</sub>O accumulation occurred due to the absence of electron acceptor. However, NO and N<sub>2</sub>O was accumulated quickly once NaNO<sub>2</sub> was added into the reactor, especially, the NO accumulation rate was much higher than that of N<sub>2</sub>O. As shown in Figs. 4 and 5, NO accumulation reached to the peak in a short time, and then decreased gradually, which maintained at a stable low level during the rest of the anoxic stage. Notably, unlike other COD/N, two peaks of NO accumulation were observed at COD/N of 6 without pH adjustment, and

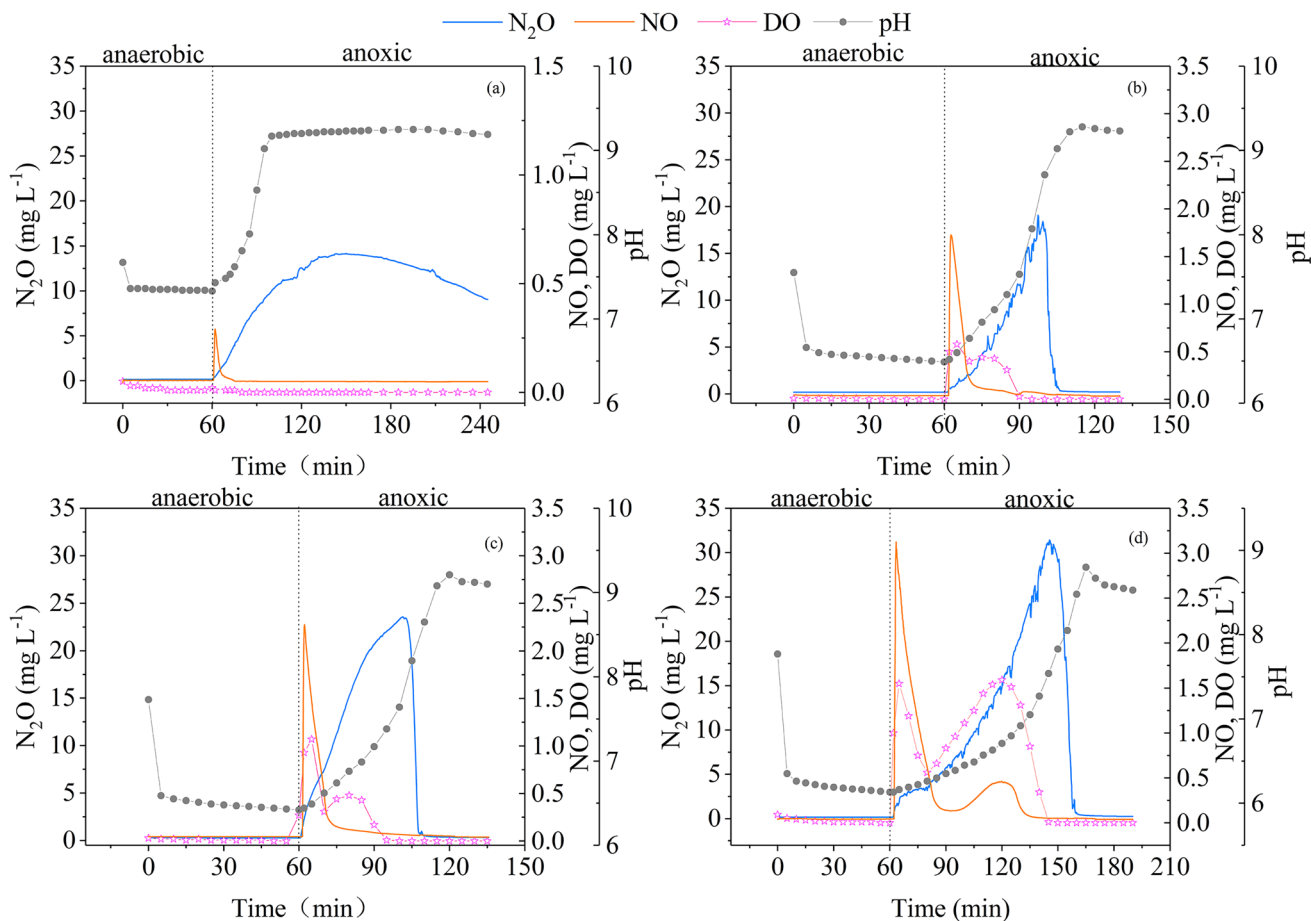


**Fig. 5** NO and N<sub>2</sub>O accumulation at different COD/N (a) COD/N=1, (b) COD/N=3, (c) COD/N=4, (d) COD/N=6

the second peak was lower than the first one, which was not found in the previous research to our best knowledge. In addition, Fig. 4, Fig. 5, and Table 2 showed that the peak and duration of NO increased and prolonged with the increase of COD/N regardless of pH adjustment, while the NO accumulation with no pH adjustment was higher than 12 times that with pH adjustment. It indicates that low COD/N and pH adjustment can mitigate NO accumulation. Interestingly, it is unexpected that high dissolved oxygen (DO) was detected

when the COD/N were 3, 4, and 6. Especially, the maximal DO of  $1.55 \pm 0.09 \text{ mg L}^{-1}$  was observed at COD/N of 6. As shown in Fig. 5, the increase of DO occurred twice under each test, namely, DO increased first and then decreased, after that, it increased again, and finally decreased to zero until the end of the test.

The results showed that the variation of N<sub>2</sub>O accumulation was different from that of NO. As shown in Fig. 5, N<sub>2</sub>O increased gradually and then decreased slowly at

**Table 2** NO and N<sub>2</sub>O production and reduction rates at different COD/N

COD/N	1	3	4	6	3a	6a
NO <sub>pro</sub> ((kg (kg vss) <sup>-1</sup> day <sup>-1</sup> )	12.94 ± 1.23	13.08 ± 3.12	16.39 ± 2.35	16.94 ± 1.98	54.45 ± 4.32	180.61 ± 11.23
NO <sub>red</sub> ((kg (kg vss) <sup>-1</sup> day <sup>-1</sup> )	10.87 ± 1.09	2.02 ± 0.21	0.88 ± 0.08	0.82 ± 0.11	53.70 ± 5.01	176.68 ± 8.99
NO <sub>max</sub> (mg L <sup>-1</sup> )	0.29 ± 0.01	1.73 ± 0.32	2.28 ± 0.21	3.12 ± 0.34	0.10 ± 0.01	0.26 ± 0.03
DO <sub>max</sub> (mg L <sup>-1</sup> )	0 ± 0	0.58 ± 0.03	1.07 ± 0.12	1.55 ± 0.09	0 ± 0	0.02 ± 0.01
N <sub>2</sub> O <sub>pro</sub> ((kg (kg vss) <sup>-1</sup> day <sup>-1</sup> )	17.05 ± 3.01	19.30 ± 2.45	13.13 ± 2.18	9.80 ± 1.02	53.48 ± 8.76	68.62 ± 4.78
N <sub>2</sub> O <sub>red</sub> ((kg (kg vss) <sup>-1</sup> day <sup>-1</sup> )	9.46 ± 1.08	10.38 ± 1.21	3.45 ± 0.45	2.14 ± 0.21	28.38 ± 1.78	63.43 ± 3.45
N <sub>2</sub> O <sub>max</sub> (mg L <sup>-1</sup> )	7.5 ± 0.78	14.12 ± 2.11	23.56 ± 1.72	31.43 ± 3.01	7.14 ± 0.67	2.64 ± 0.34
FNA <sub>max</sub> (mg L <sup>-1</sup> )	(0.7 ± 0.03) × 10 <sup>-2</sup>	(0.6 ± 0.02) × 10 <sup>-1</sup>	(0.7 ± 0.04) × 10 <sup>-1</sup>	0.15 ± 0.05	(0.1 ± 0.03) × 10 <sup>-1</sup>	(0.1 ± 0.02) × 10 <sup>-1</sup>

NO (N<sub>2</sub>O) pro: NO (N<sub>2</sub>O) production rate

NO (N<sub>2</sub>O) red: NO (N<sub>2</sub>O) reduction rate

COD/N of 1, and the  $N_2O$  decrease rate was close to that of emission rate during the decrease of  $N_2O$ , it suggests that the decrease of  $N_2O$  is mainly attributed to emission, but not biological reduction. When the COD/N was 3, 4, and 6,  $N_2O$  increased gradually at the beginning of the anoxic stage, which decreased rapidly after reaching to the peak. In addition, Fig. 5 and Table 2 showed that the peak of  $N_2O$  accumulation increased from  $7.5 \pm 0.78$  to  $31.43 \pm 3.01$  with the increase of COD/N, which was completely contrary to the previous study (Wang et al. 2019b). In addition, the results showed that there was a significant difference in  $N_2O$  accumulation between pH adjustment and non-adjustment. As shown in Fig. 4, when the pH was adjusted during the anaerobic stage,  $N_2O$  accumulation increased quickly to the peak and then decreased to the background level in a short time. The duration of  $N_2O$  accumulation with pH adjustment was much shorter than that non-adjustment. Furthermore, Table 2 showed that the peaks of  $N_2O$  accumulation (at COD/N of 3 and 6) without pH adjustment were approximately 1.98 and 11.87 times lower than that with pH adjustment.

$NO$  and  $N_2O$  emission at different COD/N are shown in Table S2. The total  $NO$  emission and  $NO$  emission factor increased with the increase of COD/N, and the maximums of  $0.99 \pm 0.11 \text{ mg L}^{-1}$  and  $1.03 \pm 0.05\%$  were achieved at COD/N of 6. It indicates that low COD/N is conducive to reduce  $NO$  emission. In addition, the results showed that compared with no pH adjustment, the total  $NO$  emission and  $NO$  emission factor decreased significantly when the pH was adjusted during the anaerobic stage. It can be calculated that  $NO$  emission factor (at COD/N of 3 and 6) without pH adjustment were approximately 2.42 and 7.92 times lower than that with pH adjustment, respectively. On the other hand, as shown in Table S2, the total  $N_2O$  emission and  $N_2O$  emission factor decreased first and then increased with the increase of COD/N, which reached to the maximums of  $3.39 \pm 0.32 \text{ mg L}^{-1}$  and  $3.50 \pm 0.45\%$  at COD/N of 1. This was different from the variation of the peak of  $N_2O$  accumulation. It is speculated that the higher  $N_2O$  emission at COD/N of 1 may be caused by the long duration of high  $N_2O$  accumulation. When the pH was adjusted during the anaerobic stage,  $N_2O$  emission factor decreased with the increase of COD/N, and the  $N_2O$  emission factor was  $0.04 \pm 0.01 \text{ mg L}^{-1}$  at COD/N of 6, which was only 0.38% of no pH adjustment. It suggests that pH adjustment has a significant effect on  $N_2O$  emission.

## Discussion

### Effect of COD/N on pollutants removal performance

In general, the CODRE will decrease with the increase of COD/N due to the excess electron donor is supplied at high

COD/N. However, in the present investigation, the lowest CODRE was observed at COD/N of 1. As stated in “Reactor setup and operation,” the pollutant removal was performed by endogenous denitrification. Therefore, the COD will be completely stored as PHAs in the anaerobic stage, and negligible biodegradable COD can be detected in the effluent (Fig. 3). It can be speculated that the difference in CODRE is mainly caused by the initial COD concentration in the influent and the non-biodegradable COD in the effluent. The results showed that the non-biodegradable COD in the effluent at different COD/N were similar, which were approximately  $30 \text{ mg L}^{-1}$ . When COD/N was 1, the initial COD was only  $100 \text{ mg L}^{-1}$ , thus, the CODRE was significantly affected by the residual non-biodegradable COD, resulting in lower CODRE. On the other hand, the non-biodegradable COD may have a slight effect on CODRE at COD/N of 3, 4, and 6 due to the high initial COD concentration in the influent. Therefore, higher CODRE was observed at high COD/N in this experiment.

The results showed that PHAs synthesis was also affected by COD/N. The amount of PHAs storage was determined by the COD concentration, namely, the higher COD was supplied, the more PHAs was stored. In addition, the results suggested that PHAs synthesis decreased slightly when pH was adjusted during anaerobic stage. Previous research has reported that the organic substance uptake is active transport, and the energy (ATP) and reducing power ( $NADH_2$ ) need to be supplied in this process. Glycolysis and tricarboxylic acid (TCA) cycle are the sources for energy and reducing power production during the anaerobic stage. However, the ATPase and fumarate reductase involve in glycolysis and TCA cycle can be inhibited by high FNA concentration, leading to insufficient energy supply. Therefore, when the FNA inhibition occurred in the reactor, more glycogen was consumed for the same organic substance uptake to meet the energy requirement. As a result, excess  $NADH_2$  was produced at the same time. In order to maintain the redox potential balance, the additional  $NADH_2$  was consumed for PHAs production through the succinate-propionate pathway. Thus, higher PHAs was detected when the pH was not adjusted during the anaerobic stage due to the high FNA concentration.

The results suggested that low COD/N was not conducive to  $NO_2^-$ -N removal, which caused a poor  $NO_2^-$ -NRE at COD/N of 1. It was calculated that the electron donor was insufficient when the COD/N is 1, so that  $NO_2^-$ -N could not be completely reduced, resulting in low removal efficiency. When the COD/N was higher than or equal to 3, the sufficient electron donor could reduce the  $NO_2^-$ -N completely. Consequently, a similar high  $NO_2^-$ -NRE was observed at different COD/N. However, there was a significant difference on the specific denitrification rate. This may be caused by the following reasons. Normally, the higher COD/N, the



faster denitrification rate due to sufficient electron donor. It was also verified in this experiment with pH adjustment during the anaerobic stage. However, a different trend was observed when the pH was not adjusted. As shown in Fig. 3, the  $\text{NO}_2^-$ -N reduction rate decreased with the increase of COD/N at the beginning of the anoxic stage. Literatures have showed that the denitrifier activity could be inhibited when FNA concentration was  $0.001 \sim 0.039 \text{ mg L}^{-1}$  (Abeling and Seyfried 1992; Glass et al. 1997; Ma et al. 2010). As shown in Table 2, the FNA concentrations at COD/N of 3, 4, 6 at the beginning of the anoxic stage were  $(0.6 \pm 0.02) \times 10^{-1}$ ,  $(0.7 \pm 0.04) \times 10^{-1}$ , and  $0.15 \pm 0.05 \text{ mg L}^{-1}$ , respectively, which were higher than the range of FNA inhibition on denitrifier. Therefore, it is speculated that the denitrification may be inhibited by the FNA. Baumann et al. (1997) has reported that the translation of Nir mRNA can be inhibited by FNA, resulting in the synthesis of reductase is folded and translocated improperly, or the synthesized reductase become inactivated (Baumann et al. 1997). Furthermore, the conformation of Nir also can be changed by the high FNA concentration. Subsequently, the Nir activity decreased, which could lead to the reduction of the specific denitrification rate directly. On the other hand, it is known that the adenosine diphosphate (ADP), Pi and ATP in microbial cells can regulate each other. When ATP is high, the amounts of ADP and adenosine phosphate (AMP) will decrease. The oxidative phosphorylation and TCA cycle rate also slow down, and ATP synthesis decreases. In this experiment, high FNA concentration inhibited the microbial growth, leading to a reduction in the microbial energy demand, as a result, the ATP accumulation occurred in this stage. Therefore, the intracellular ADP concentration decreased, which would slow down the ATP synthesis, and subsequently reduced the denitrification rate. In addition, NO accumulation also has an important effect on specific denitrification rate. Previous research has reported that NO is a potent toxic substance that can exert severe effects on the metabolism of bacteria (Wang et al. 2016), and the inhibition thresholds of NO on Nir, Nor, and Nos were 0.5, 0.3, and  $0.075 \text{ mg L}^{-1}$ , respectively (Ni and Yuan 2013). In the present experiment, the peaks of NO accumulation at COD/N of 3, 4, and 6 were  $1.73 \pm 0.32$ ,  $2.28 \pm 0.21$ , and  $3.12 \pm 0.34 \text{ mg L}^{-1}$ , respectively, which were much higher than the inhibition thresholds that reported in literature (Ni and Yuan 2013). Therefore, it indicates that the slow specific denitrification rate at the beginning of the anoxic stage has a close relationship with NO accumulation.

## Mechanism of NO and $\text{N}_2\text{O}$ accumulation

### Mechanism of NO accumulation

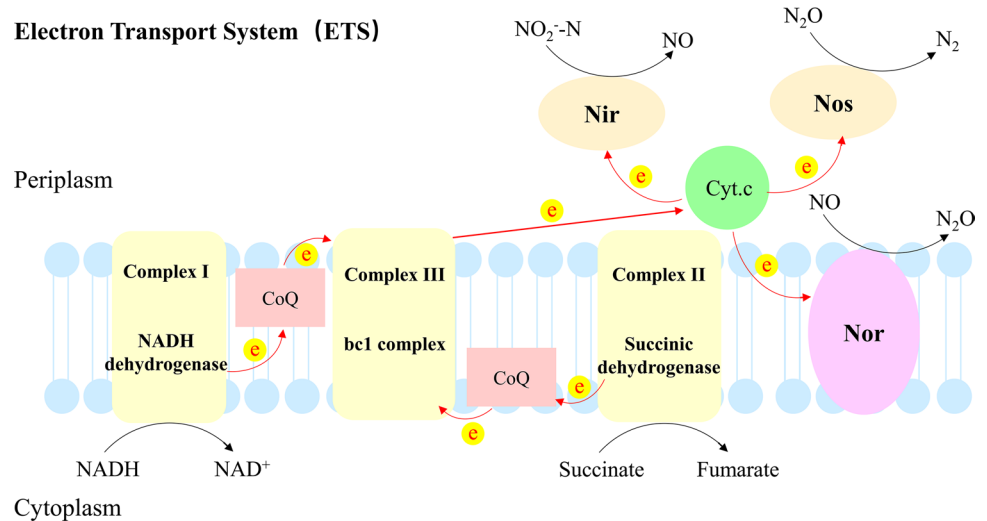
Microbial denitrification is the electron-driven biochemical reaction. Thus, the electron behaviors (production, transport

and consumption) play crucial role in denitrification. Previous research has reported that electron production, transport, and consumption is usually performed in the electron transport system (ETS). In this system, electrons are produced by NADH dehydrogenase (complex I) and succinate dehydrogenase (complex II), then transferred by quinone pool (CoQ), bc1 complex (complex III), and cytochrome c (Cyt c), and finally utilized by the reductases (Nar, Nir, Nor, and Nos) (Fig. 6). Therefore, it can be concluded that the activity of reductases has a significant effect on electron transport and consumption. In general, the electrons are consumed evenly by the reductases, and no intermediate is accumulated in the denitrification. However, when the activity of reductases is seriously affected by the operation condition or some inhibitors, the electron transport and consumption may be hampered, which can result in imbalanced electron distribution. Consequently, the intermediates, such as NO and  $\text{N}_2\text{O}$ , may be accumulated in this process.

In this experiment, the activity of reductases involved in the denitrification decreased significantly after suffering a 60-min anaerobic stage due to the lack of electron acceptor for a long time. As a result, the electron transport and consumption were hampered, and the  $\text{NO}_2^-$ -N could not successfully transfer to  $\text{N}_2$  as usual when the  $\text{NaNO}_2$  was added at the beginning of the anoxic stage. Bao et al. (2018) has reported that the recovery of reductase activity can be stimulated and improved by its related substrates. Therefore, when the  $\text{NO}_2^-$ -N was supplied in the reactor, the Nir activity was recovered firstly, resulting in the rapid  $\text{NO}_2^-$ -N reduction at the beginning of the anoxic stage. Subsequently, high NO accumulation was observed at this stage. On the other hand, NO accumulation stimulated the recovery of Nor activity, and then NO was reduced to  $\text{N}_2\text{O}$  in the following stage.

In addition, FNA and NO inhibition played significant roles in NO accumulation, results showed that the correlation coefficients of FNA and NO accumulation at different COD/N were higher than 0.90 (data not shown). The inhibition mechanisms of FNA are as follows. Firstly, it is known that FNA is an uncoupler that can passively diffuse across the cell membrane, shuttling protons on both sides of the cell membrane without producing energy, which may lead to the collapse of proton motive force (PMF) (Chislett et al. 2022). Subsequently, the ATP synthesis is inhibited and the metabolism activity of the bacteria decreased simultaneously. Secondly, previous research has reported that FNA can directly react with the enzymes involved in microbial metabolism (Park 1993). The sulfhydryl (SH)-containing enzymes (such as CoA-SH) are important part in TCA cycle, which can be inhibited by reacting with FNA (Zhou et al. 2011). This reaction has a negative impact on the energy production process of the cell, because NADH produced by TCA is subsequently converted into ATP. Furthermore, FNA also can react with glyceraldehyde-3-phosphate dehydrogenase

**Fig. 6** Schematic diagram of electron transport system in nitrite denitrification



that involved in glycolysis, resulting in the inactivation of the enzyme (Zhou et al. 2010). Thirdly, the Nor can be inhibited directly by FNA, which will lead to NO cannot be efficiently reduced to  $N_2O$ . As a result, the intermediate of NO may be accumulated in the denitrification. NO is a well-known cytotoxin, which can react with metal centers of proteins and heme to form nitroso complexes. The copper-sulfide proteins are crucial units in ATP production and electron transfer. Therefore, the destruction of enzyme catalytic sites and the formation of complex will severely inhibit electron transfer, resulting in the accumulation of intermediate. In addition, it has reported that Nor can be inhibited by NO, and the inhibition threshold is  $0.3 \text{ mg L}^{-1}$ . In this experiment, the NO accumulation at COD/N of 3, 4, and 6 without pH adjustment were significantly higher than the threshold. It indicates that NO inhibition is an important reason for high NO accumulation.

The results showed that NO emission and the peak of NO accumulation increased with the increase of COD/N. It is well-known that NO accumulation is determined by its production rate ( $\text{NO}_2^-$ -N reduction rate), reduction rate, and emission rate. In this study, the same reactor and operation condition was supplied in the batch test, there was no significant difference on NO emission rate at different COD/N. Therefore, the NO accumulation was only determined by NO production rate and reduction rate. As shown in Table 2, NO production rate increased with the increase of COD/N when the pH was not adjusted during the anaerobic stage. However, the NO reduction rate showed an opposite trend with its production rate. The different variation may be caused by the following reason. It is known that the pH decreases during the PHAs synthesis, and the more PHAs is synthesized, the greater the decrease of pH. In addition, acetate was used as the carbon source in this experiment, high acetate concentration could lead to low pH due to its acidity.

These led to higher FNA was accumulated at the beginning of the anaerobic stage at high COD/N when the pH was not adjusted during the anaerobic stage. Therefore, the Nor activity was significantly inhibited by the FNA. As a result, the NO reduction rate decreased with the increase of COD/N. As shown in Figs. S1 and S2, the electron distribution and electron consumption rate of Nor decreased from 40.11% and  $0.78 \text{ mol g}^{-1} \text{ day}^{-1}$  to 4.62% and  $0.06 \text{ mol g}^{-1} \text{ day}^{-1}$  when the COD/N increased from 1 to 6. However, Figs. S1 and S2 showed that the electron distribution and electron consumption rate of Nir increased from 47.75% and  $0.92 \text{ mol g}^{-1} \text{ day}^{-1}$  to 95.31% and  $1.21 \text{ mol g}^{-1} \text{ day}^{-1}$  respectively with the increase of COD/N. It indicates that Nir activity is not affected by FNA inhibition. The results suggested that the imbalanced electron distribution was intensified with the increase of COD/N due to the different FNA inhibition on reductases. Therefore, the serious imbalanced electron distribution led to a higher NO accumulation was observed at high COD/N with no pH adjustment.

On the other hand, when the pH was adjusted during the anaerobic stage, the similar pH was observed at the beginning of the anaerobic stage, and the FNA concentration was lower than the inhibition threshold. Thus, the NO accumulation was only affected by COD/N. Table 2 showed that the NO reduction rate increased with the increase of COD/N as its production rate, while the increase range was smaller than that of production rate. Fig. S1 showed that the electron consumption rates of Nir and Nor increased by 9.02 and  $8.79 \text{ mol g}^{-1} \text{ day}^{-1}$ , respectively when COD/N increased from 3 to 6a. It indicates that the Nir can capture more electrons than Nor when the sufficient electrons are supplied. This led to high NO accumulation occur at high COD/N. Therefore, the NO accumulation with pH adjustment also increased with the increase of COD/N.

Figure 5d showed that two peaks of NO accumulation were observed during nitrite denitrification. It speculated that the possible reasons are as follow. Nir and Nor might be inhibited completely when NO accumulation reached to the peak, and the decrease of NO was partially attribute to emission. Meanwhile, in order to mitigate the NO toxicity, microorganism would convert the NO to other substances by another pathway (details are discussed in “Mechanism of NO detoxification”), resulting in the decrease of NO. When NO reached to a low level, the reductases involved in denitrification were recovered gradually. Literature showed that Nos was most sensitive to NO toxicity, followed by Nor, and finally Nir (Ni and Yuan 2013). Therefore, the recovery of Nir activity was easier than that of Nor, resulting in the NO accumulation again. After that, NO decreased again due to detoxification by microorganisms and emission. However, it can be observed that the second NO accumulation was much lower than the first one. It suggests that the activities of reductases have been recovered partly. After a period of adaptation, the activities of reductases were recovered completely, NO accumulation would not occur, and maintained at a very low level.

### Mechanism of NO detoxification

In this experiment, NO detoxification pathways included three parts: NO emission, NO reduction, and NO dismutation. As is known to all, NO is poorly soluble in water, which will emit from the reactor with agitation when it accumulated in the denitrification. Therefore, NO emission is a significant process for NO detoxification.

It is commonly known that high NO accumulation has a serious effect on the reductases involved in denitrification, leading to low denitrification rate. Therefore, when the NO accumulation occurs in the denitrification, the microorganism will rapidly transform the NO to other non-toxic substance, such as  $N_2O$ , to mitigate the toxicity. However, the Nor activity can be inhibited completely once the NO accumulation reach to a very high level, which result in NO cannot be reduced to  $N_2O$ . Previous research has showed that the inhibition threshold of NO on Nor is  $0.3 \text{ mg L}^{-1}$  (Ni and Yuan 2013). In this experiment, the peaks of NO accumulation at COD/N of 3, 4, 6 were much higher than the reported threshold. It indicates that the NO reduction may be inhibited significantly by the high NO accumulation, leading to part of NO cannot be reduced to  $N_2O$  as usual. It is noteworthy that a novel NO transformation pathway, NO dismutation ( $2NO = N_2 + O_2$ ), has been proposed in recent years. Ettwig et al. (2010) found that NO was not reduced to  $N_2O$  during nitrite-driven anaerobic methane oxidation (n-DAMO) (Ettwig et al. 2010). Instead, it was dismutated to  $N_2$  and  $O_2$  by the putative NO dismutase (Nod). In addition, researches show that the Nod has been detected in wastewater, wetland, and hydrocarbon-contaminated soil,

indicating that there is a high diversity and distribution of Nod in the different ecosystems (Hu et al. 2019; Lichtenberg et al. 2021; Zhang et al. 2021). In this experiment, high DO of  $0.58 \pm 0.03$ ,  $1.07 \pm 0.12$ ,  $1.55 \pm 0.09 \text{ mg L}^{-1}$  were detected at different COD/N of 3, 4, 6 without pH adjustment. Therefore, it is speculated that the high DO may have a close relationship with NO dismutation. However, literature showed that the NO can causes a positive inference on the readings of some models of DO sensors, including YSI 5178, YSI FDO 70×IQ (SW), and Hach LDO 101 (Klaus et al. 2017). The DO sensor used in present experiment was HACH HQ30d, which also might be interfered by NO. Thus, some interference tests were performed to determine this speculation (data no shown). The results showed that the DO sensor of HACH HQ30d was interfered by NO. Therefore, the high DO detected in this experiment may also be related to the NO interference. Based on the above analysis, it is difficult to determine whether the DO is caused by NO interference or NO dismutation. Therefore, an abiotic test was conducted to clarify the source of high DO readings, the details of the test was performed according to Wang et al. (2019b). Then, the interfering and real DO could be calculated by the correlation equation. Figure S3 showed that the detected DO in COD/N of 3, 4, and 6 without pH adjustment were higher than the interfering DO, especially, high DO accumulation of  $1.39 \text{ mg L}^{-1}$  was observed at the final stage of NO accumulation. It indicated that NO dismutation occurred in this experiment, and which might be the main pathway of NO detoxification during final stage of NO accumulation. The possible reasons are concluded as follows. In the denitrification, the main enzyme for NO reduction is Nor. In generally, the Nor activity is higher than that of Nod when NO is accumulated in the reactor. Therefore, at the beginning of the NO accumulation stage, most of NO was reduced to  $N_2O$ , and only a small part of NO was transformed to  $N_2$  and  $O_2$ . However, when the NO reached to a high level, Nor and Nod activities were inhibited, NO reduction and dismutation rates decreased, resulting in slow  $N_2O$  accumulation rate and decrease of DO. With the decrease of NO accumulation, Nor and Nod activities recovered gradually, and the recovery of Nod activity was faster than Nor due to the sensitivity of Nor to NO. Thus, in this stage, the NO was primary transformed by NO dismutation, DO increased again, and which was higher than the first time. After a period of adjustment, Nor activity recovered completely, the NO was reduced to  $N_2O$  as usual. In this process, the NO dismutation in NO detoxification was decreased gradually.

### Mechanism of $N_2O$ accumulation

As shown in Figs. 3 and 4, high  $N_2O$  concentration accumulated at different COD/N, which may be affected by three

factors, including FNA concentration, NO concentration, and COD/N.

It is known that FNA is a significant inhibitor on  $N_2O$  reduction due to the high sensitivity of Nos on FNA (Zhou et al. 2022). Literature showed that the FNA inhibition threshold on Nos was  $0.004 \text{ mg L}^{-1}$  (Zhou et al. 2008). In this experiment, the highest FNA concentration at different COD/N (1, 3, 4, 6, 3a, 6a) were 0.007, 0.06, 0.07, 0.15, 0.01, and  $0.01 \text{ mg L}^{-1}$  respectively, which were higher than the inhibition threshold. Therefore, it indicates that FNA inhibition played an important role in  $N_2O$  accumulation in present experiment. The inhibition mechanisms of FNA on  $N_2O$  reduction are as follows. On the one hand, FNA can react directly with Nos. Nos has two metal centers: CuA, a binuclear copper center, which is used to receive and transfer electrons; CuZ, a tetranuclear copper-sulfide center, which contains one or two sulfide bridges (Guo et al. 2017). FNA can bind to the active sites of copper-contained enzymes (Nos), leading to Nos inactivation or incomplete biosynthesis. As a result, the  $N_2O$  reduction will suffer a competitive inhibition. On the other hand, FNA has an adverse effect on the translation and expression of Nos gene. Previous research showed that high FNA concentration could inhibit the translation of Nos mRNA, or improperly translocate and fold the Nos (Baumann et al. 1997). They believed that the inactivation of the synthesized enzyme and/or the conformational change by the high FNA concentration also could inhibit Nos activity, so that  $N_2O$  could not reduce to  $N_2$ .

Another important reason for  $N_2O$  accumulation is electron competition caused by insufficient electron supply. Literature has reported that Nir, Nor, and Nos receive electrons from the same cytochrome (Richardson et al. 2009). Therefore, the electron competition among these reductases may occur once the electron cannot meet the requirements for electrons by denitrification, and Nos is the weakest competitor with a lower affinity for electron donor than Nir and Nor (Guo et al. 2017). In this experiment, the electron donors were supplied from PHAs oxidation process. Compared with exogenous organic matter, the difficult degradation of PHAs may not supply enough electron donors for denitrification. As a result, the electron competition will intensify, and  $N_2O$  reduction is inhibited due to the lowest electron capture ability of Nos. In addition, COD/N also plays a significant role in  $N_2O$  accumulation. In the test of COD/N of 1, the electron donor was severely insufficient to reduce  $N_2O$ , resulting in high  $N_2O$  accumulation. Especially, there was no electron donor to reduce  $N_2O$  at the final stage of denitrification, and the reduction of  $N_2O$  is mainly caused by emission. When the pH was adjusted during the anaerobic stage, there was no different factors affecting  $N_2O$  accumulation except COD/N. Table 2 showed that the maximal  $N_2O$  accumulation decreased with the increase of COD/N. Therefore, it can

be concluded that low COD/N promotes  $N_2O$  accumulation due to the more severe electron competition.

$N_2O$  accumulation is also related to NO inhibition. NO is a cytotoxin, which has a serious effect on enzyme and microorganism. As stated in previous section, metal centers of CuA and CuZ are contained in Nos. Research has reported that CuZ is susceptible to NO, which can inactivate it significantly (Richardson et al. 2009). If the CuZ is destroyed, the electrons cannot be transferred to Nos and used by it, resulting in  $N_2O$  rather than  $N_2$  as the end product in nitrite denitrification. On the other hand, it has been reported that cytochrome c is able to bind NO in denitrification at the physiological concentration of  $10^{-9} \sim 10^{-7} \text{ mol L}^{-1}$  (Goretski et al. 1990). Carr and Ferguson (1990) found that the activity of cytochrome oxidase was hindered by high NO, which led to a serious inhibition (Carr and Ferguson 1990). Furthermore, Yu et al. (2019) reported that the conformation of cytochrome c was changed by NO, causing the decrease of Nos activity and loss of electron transfer (Yu et al. 2019). Consequently, the electron competition among Nir, Nor, and Nos intensified, and high  $N_2O$  accumulation occurred in the experiment.

The results showed that the peak of  $N_2O$  accumulation increased with the increase of COD/N when pH was not adjusted during the anaerobic stage, while an opposite trend was observed with pH adjustment. It was caused by the different inhibitions on  $N_2O$  reduction under different conditions. When pH was adjusted during the anaerobic stage, the  $N_2O$  accumulation was mainly affected by COD/N, there was little inhibition occurred. The Nos activity was high, resulting in high electron consume rates ( $2.03$  and  $4.5 \text{ mol g}^{-1} \text{ day}^{-1}$ ) at COD/N of 3a and 6a, and low  $N_2O$  was accumulated. In addition, the more electron was supplied, the lower  $N_2O$  was accumulated. When COD/N was 1, the FNA and NO concentration was low, but the electron donor was insufficient, which could intensify electron competition, the electron consume rate of Nos was only  $0.75 \text{ mol g}^{-1} \text{ day}^{-1}$ , leading to high  $N_2O$  accumulation. As shown in Table 2, high NO and FNA concentration were detected at COD/N of 3, 4, 6, which had serious effect on Nos. Figure S4 showed that the electron consume rates of Nos at COD/N of 3, 4, 6 decreased to 0.74, 0.25, and  $0.22 \text{ mol g}^{-1} \text{ day}^{-1}$ , respectively. Consequently, the  $N_2O$  accumulation increased with the increase of COD/N. Furthermore, as stated before, the intermediate accumulation during nitrite denitrification is closely related to electron distribution. Figure S5 showed that the differences of electron distribution between Nor and Nos at different COD/N (1, 3, 4, 6, 3a, 6a) were 15.78, 18.17, 26.41, 29.04, 15.54, and 2.58%, respectively. Therefore, it was further suggested that the imbalanced electron distribution between Nor and Nos caused by COD/N, FNA and NO inhibition resulted in the different  $N_2O$  accumulation.



## Conclusion

The mechanisms of NO and N<sub>2</sub>O accumulation, as well as NO detoxification were investigated in this study, the main conclusions are as follows.

- (1) CODRE increased with the increase of COD/N, which was closely related to influent COD concentration and the residual non-biodegradable COD in the effluent. High NO<sub>2</sub><sup>-</sup>-NRE (> 99%) was achieved when COD/N was higher than 1 because of the sufficient electron donors.
- (2) NO accumulation was affected by anaerobic time, COD/N, FNA, and NO concentration. The Nos activity can be reduced by anaerobic time, FNA and NO, and the electron transport and distribution is hindered, resulting in imbalanced electron distribution, and the NO accumulation occurred. More electrons can be applied for reduction of NO<sub>2</sub><sup>-</sup>-N to NO at high COD/N, leading to high NO accumulation was observed at high COD/N.
- (3) There were three pathways of NO detoxification, which were NO emission, reduction and dismutation. The more NO produced, the more proportion of NO dismutation pathway. The maximal DO concentration during NO dismutation in this study was 1.39 mg L<sup>-1</sup>.
- (4) N<sub>2</sub>O accumulation increased with the increase of COD/N without pH adjustment, while an opposite trend was observed when pH was adjusted. It is mainly attributed to FNA and NO inhibition. Sufficient electron can be supplied for N<sub>2</sub>O reduction at high COD/N, but the high FNA and NO concentration caused by no pH adjustment will inhibit Nos activity and hinder the reduction of N<sub>2</sub>O to N<sub>2</sub>.

**Supplementary Information** The online version contains supplementary material available at <https://doi.org/10.1007/s11356-022-24874-w>.

**Author contribution** All authors contributed to the study conception and design. Material preparation was performed by Bin Li. Data collection and analysis were performed by Fang Li. The first draft of the manuscript was written by Sha Wang and all authors commented on previous versions of the manuscript. All authors read and approved the final manuscript.

**Funding** This work was supported by the Scientific Research Program Funded by Shaanxi Provincial Education Department (No. 21JK0638) and Talent Project of Weinan Normal University (No. 2021RC27).

**Data availability** The datasets used or analyzed during the current study are available from the corresponding author on reasonable request.

## Declarations

**Conflict of interest** The authors declare no competing interests.

## References

- Abeling U, Seyfried CF (1992) Anaerobic-aerobic treatment of high strength ammonium wastewater nitrogen removal via nitrite. *Water Sci Technol* 26:1007–1015. <https://doi.org/10.2166/wst.1992.0542>
- Adouani N, Lendormi T, Limousy L, Sire O (2010) Effect of the carbon source on N<sub>2</sub>O emissions during biological denitrification. *Resour Conserv Recy* 54:299–302. <https://doi.org/10.1016/j.resconrec.2009.07.011>
- APHA (2005) Standard methods for the examination of water and wastewater. American Public Health Association (APHA), Washington DC
- Bao Z, Ribera-Guardia A, Spinelli M, Sun D, Pijuan M (2018) The effect of temperature shifts on N<sub>2</sub>O and NO emissions from a partial nitrification reactor treating reject wastewater. *Chemosphere* 212:162–169. <https://doi.org/10.1016/j.chemosphere.2018.08.090>
- Baumann B, Meer JRvd, Snozzi M, Zehnder AJB (1997) Inhibition of denitrification activity but not of mRNA induction in *Paracoccus denitrificans* by nitrite at a suboptimal pH. *Anton Leeuw Int J G* 72:183–189. <https://doi.org/10.1023/A:1000342125891>
- Carr GJ, Ferguson SJ (1990) Nitric oxide formed by nitrite reductase of *Paracoccus denitrificans* is sufficiently stable to inhibit cytochrome oxidase activity and is reduced by its reductase under aerobic conditions. *Bba-Biomembranes* 1017:57–62. [https://doi.org/10.1016/0005-2728\(90\)90178-7](https://doi.org/10.1016/0005-2728(90)90178-7)
- Chislett M, Guo J, Bond PL, Wang Y, Donose BC, Yuan Z (2022) Reactive nitrogen species from free nitrous acid (FNA) cause cell lysis. *Water Res* 217:118401. <https://doi.org/10.1016/j.watres.2022.118401>
- Dehghani S, Rezaee A, Hosseinkhani S (2018) Effect of alternating electrical current on denitrifying bacteria in a microbial electrochemical system: biofilm viability and ATP assessment. *Environ Sci Pollut Res* 25:33591–33598. <https://doi.org/10.1007/s11356-018-3170-0>
- Dobbeleers T, Caluwé M, Daens D, Geuens L, Dries J (2018) Evaluation of two start-up strategies to obtain nitrogen removal via nitrite and examination of the nitrous oxide emissions for different nitrification levels during the treatment of slaughterhouse wastewater. *J Chem Technol Biot* 93:569–576. <https://doi.org/10.1002/jctb.5403>
- Ettwig KF et al (2010) Nitrite-driven anaerobic methane oxidation by oxygenic bacteria. *Nature* 464:543–548. <https://doi.org/10.1038/nature08883>
- Fu K, Zhang X, Liu F, Qiu F, Cao X (2021) Effect of C/N on denitrification and N<sub>2</sub>O release with glucose as the carbon source. *Chin J Environ Eng* 15:1279–1288 (in Chinese)
- Glass CC, Silverstein J, Oh J (1997) Inhibition of denitrification in activated sludge by nitrite. *Water Environ Res* 69:1086–1093. <https://doi.org/10.2175/106143097X125803>
- Goretski J, Zafiriou OC, Hollocher TC (1990) Steady-state nitric oxide concentrations during denitrification. *J Biol Chem* 265:11535–11538. [https://doi.org/10.1016/S0021-9258\(19\)38430-3](https://doi.org/10.1016/S0021-9258(19)38430-3)
- Guo G, Wang Y, Hao T, Wu D, Chen G-H (2017) Enzymatic nitrous oxide emissions from wastewater treatment. *Front Environ Sci Eng* 12:10. <https://doi.org/10.1007/s11783-018-1021-3>
- Hossini H, Rezaee A, Ayati B, Mahvic A (2015) Simultaneous nitrification and denitrification using a polypyrrole/microbial cellulose electrode in a membraneless bio-electrochemical system. *RSC Adv* 5:72699–72708. <https://doi.org/10.1039/C5RA09771A>
- Hu QQ, Zhou ZC, Liu YF, Zhou L, Mu BZ (2019) High microbial diversity of the nitric oxide dismutation reaction revealed by PCR



- amplification and analysis of the nod gene. *Int Biodeter Biodegr* 143:104708. <https://doi.org/10.1016/j.ibiod.2019.05.025>
- IPCC (2013) Fifth Assessment Report, Climate Change 2013 The Physical Science Basis. Stockholm, Sweden
- Jia W, Liang S, Ngo HH, Guo W, Zhang J, Wang R, Zou Y (2013) Effect of phosphorus load on nutrients removal and N<sub>2</sub>O emission during low-oxygen simultaneous nitrification and denitrification process. *Bioresour Technol* 141:123–130. <https://doi.org/10.1016/j.biortech.2013.02.095>
- Jonoush ZA, Rezaee A, Ghaffarinejad A (2020) Electrocatalytic nitrate reduction using Fe<sup>0</sup>/Fe<sub>3</sub>O<sub>4</sub> nanoparticles immobilized on nickel foam: selectivity and energy consumption studies. *J Clean Prod* 242:118569–118581. <https://doi.org/10.1016/j.jclepro.2019.118569>
- Klaus S, Sadowski M, Jimenez J, Wett B, Chandran K, Murthy S, Bott CB (2017) Nitric oxide production interferes with aqueous dissolved oxygen sensors. *Environ Eng Sci* 3:687–691. <https://doi.org/10.1089/ees.2016.0634>
- Lichtenberg M, Line L, Schrameyer V, Jakobsen TH, Rytke ML, Toyofuku M, Nomura N, Kolpen M, Tolker-Nielsen T, HI MK, Bjarnsholt T (2021) Nitric-oxide-driven oxygen release in anoxic *Pseudomonas aeruginosa*. *iScience* 24:103404. <https://doi.org/10.1016/j.isci.2021.103404>
- Ma J, Yang Q, Wang S, Wang L, Takigawa A, Peng Y (2010) Effect of free nitrous acid as inhibitors on nitrate reduction by a biological nutrient removal sludge. *J Hazard Mater* 175:518–523. <https://doi.org/10.1016/j.jhazmat.2009.10.036>
- Ni BJ, Yuan Z (2013) A model-based assessment of nitric oxide and nitrous oxide production in membrane-aerated autotrophic nitrogen removal biofilm systems. *J Membrane Sci* 428:163–171. <https://doi.org/10.1016/j.memsci.2012.10.049>
- Pan Y, Ni BJ, Bond PL, Ye L, Yuan Z (2013) Electron competition among nitrogen oxides reduction during methanol-utilizing denitrification in wastewater treatment. *Water Res* 47:3273–3281. <https://doi.org/10.1016/j.watres.2013.02.054>
- Park JW (1993) S-nitrosylation of sulfhydryl groups in albumin by nitrosating agents. *Arch Pharm Res* 16:1–5. <https://doi.org/10.1007/BF02974119>
- Richardson D, Felgate H, Watmough N, Thomson A, Baggs E (2009) Mitigating release of the potent greenhouse gas N<sub>2</sub>O from the nitrogen cycle - could enzymic regulation hold the key? *Trends Biotechnol* 27:388–397. <https://doi.org/10.1016/j.tibtech.2009.03.009>
- Schulthess RV, Kühni M, Gujer W (1995) Release of nitric and nitrous oxides from denitrifying activated sludge. *Water Res* 29:215–226. [https://doi.org/10.1016/0043-1354\(94\)E0108-I](https://doi.org/10.1016/0043-1354(94)E0108-I)
- Wang Y, Lin X, Zhou D, Ye L, Han H, Song C (2016) Nitric oxide and nitrous oxide emissions from a full-scale activated sludge anaerobic/anoxic/oxic process. *Chem Eng J* 289:330–340. <https://doi.org/10.1016/j.watres.2007.08.022>
- Wang S, Zhao J, Ding X, Zhao R, Huang T, Lan L, Naim Bin Nasry AA, Liu S (2019a) Effect of starvation time on NO and N<sub>2</sub>O production during heterotrophic denitrification with nitrite and glucose shock loading. *Process Biochem* 86:108–116. <https://doi.org/10.1016/j.procbio.2019.07.023>
- Wang S, Zhao J, Huang T (2019b) High NO and N<sub>2</sub>O accumulation during nitrite denitrification in lab-scale sequencing batch reactor: influencing factors and mechanism. *Environ Sci Pollut Res* 26:34377–34387. <https://doi.org/10.1007/s11356-019-06391-5>
- Yu C, Qiao S, Yang Y, Jin R, Zhou J, Rittmann BE (2019) Energy recovery in the form of N<sub>2</sub>O by denitrifying bacteria. *Chem Eng J* 371:500–506. <https://doi.org/10.1016/j.cej.2019.04.015>
- Zhang D, Han X, Zhou S, Yuan S, Lu P, Peng S (2021) Nitric oxide-dependent biodegradation of phenanthrene and fluoranthene: the co-occurrence of anaerobic and intra-aerobic pathways. *Sci Total Environ* 760:144032. <https://doi.org/10.1016/j.scitotenv.2020.144032>
- Zhou Y, Pijuan M, Zeng RJ, Yuan Z (2008) Free nitrous acid inhibition on nitrous oxide reduction by a denitrifying-enhanced biological phosphorus removal sludge. *Environ Sci Technol* 42:8260–8265. <https://doi.org/10.1021/es800650j>
- Zhou Y, Ganda L, Lim M, Yuan Z, Kjelleberg S, Ng WJ (2010) Free nitrous acid (FNA) inhibition on denitrifying poly-phosphate accumulating organisms (DPAOs). *Appl Microbiol Biotechnol* 88:359–369. <https://doi.org/10.1007/s00253-010-2780-3>
- Zhou Y, Oehmen A, Lim M, Vadivelu V, Ng WJ (2011) The role of nitrite and free nitrous acid (FNA) in wastewater treatment plants. *Water Res* 45:4672–4682. <https://doi.org/10.1016/j.watres.2011.06.025>
- Zhou Y, Zhao S, Suenaga T, Kuroiwa M, Riya S, Terada A (2022) Nitrous oxide-sink capability of denitrifying bacteria impacted by nitrite and pH. *Chem Eng J* 428:132402. <https://doi.org/10.1016/j.cej.2021.132402>

**Publisher's note** Springer Nature remains neutral with regard to jurisdictional claims in published maps and institutional affiliations.

Springer Nature or its licensor (e.g. a society or other partner) holds exclusive rights to this article under a publishing agreement with the author(s) or other rightsholder(s); author self-archiving of the accepted manuscript version of this article is solely governed by the terms of such publishing agreement and applicable law.